

# Fingerprints of Disorder Source in Graphene

P. Zhao,<sup>1</sup> S. Yuan,<sup>2,\*</sup> M. I. Katsnelson,<sup>2</sup> and H. De Raedt<sup>1</sup>

<sup>1</sup>*Department of Applied Physics, Zernike Institute for Advanced Materials, University of Groningen, Nijenborgh 4, NL-9747AG Groningen, The Netherlands*

<sup>2</sup>*Radboud University of Nijmegen, Institute for Molecules and Materials, Heijendaalseweg 135, 6525 AJ Nijmegen, The Netherlands*

(Dated: December 3, 2024)

We present a systematic study of the electronic, transport and optical properties of disordered graphene including the next-nearest-neighbor hopping. We show that this hopping has a non-negligible effect on resonant scattering but is of minor importance for long-range disorder such as charged impurities, random potentials or hoppings induced by strain fluctuations. Different types of disorder can be recognized by their fingerprints appearing in the dc conductivity, carrier mobility, optical spectroscopy and Landau level spectrum. By matching our calculations to the experimental observations, we conclude that the long-range disorder potential induced by strain is the most important source of disorder in high-quality graphene on a substrate.

PACS numbers: 72.80.Rj; 73.20.Hb; 73.61.Wp

The dominant source of disorder which limits the transport and optical properties of graphene is still under debate. Different mechanisms have been proposed and investigated intensively, including charged impurities, random strain fluctuations and resonant scatterers (for reviews see Refs. 1 and 2). Early on, charged impurities (CI) have been recognized as the dominate disorders due to graphene's unusual linear carrier-density-dependent conductivity. However, this mechanism does not explain the experimental observations that the transport properties are not sensitive to the substrate screening [3, 4]. On the other hand, charge inhomogeneities due to strain fluctuations (SF) form electron-hole puddles [5–7] and there is experimental evidence, based on the correlation between the carrier mobility and the width of the resistance peak around charge neutrality, that the long-range disorder potential (LRDP) due to SF could be the dominant source of disorder in high-quality graphene on a substrate [8]. In addition, the SF modulate the electron hopping energies between different atomic sites, inducing the long-range disorder hopping (LRDH), leading to the appearance of the (pseudo) vector potential [2, 9]. Another common source of disorder are resonant scatterers (RS) such as chemical species like hydrogen or organic groups, which also lead to a sublinear carrier-density-dependent conductivity and a minimum conductivity plateau around the neutrality point [10, 11].

Besides the transport properties, an important part of our knowledge about the electronic properties derives from the optical spectroscopy measurements [1, 12]. Infrared spectroscopy experiments allow for the control of interband excitations by means of electrical gating [13, 14]. For doped pristine graphene with nonzero chemical potential  $\mu_F$ , the optical conductivity is a step function  $\sigma(\omega) = \sigma_0 \Theta(\omega - 2\mu_F)$  at zero temperature due to Pauli's exclusion principle. However, there are experimentally observed background contributions to the op-

tical spectroscopy between  $0 < \omega < 2\mu_F$  [15, 16], which are due to the extra intraband excitations introduced by disorder or many-body effects [14, 17–27]. This opens the possibility to identify the source of disorder via the optical measurements.

Previous theoretical investigation of disorders are mainly based on models without considering the next-nearest-neighbor (NNN) hopping  $t'$ . The breakdown of electron-hole symmetry resulting from  $t' \neq 0$  shifts the position of Dirac point from zero to  $3t'$  [2, 28]. Recent quantum capacitance measurements indicate that the value of  $t'$  is about 0.3eV [29], consistent with the values obtained from the density functional calculations. It is generally thought that  $t'$  has relatively weak effects on the physical properties of graphene at low energies [2, 23, 28, 29]. In this letter we show that including  $t'$  has a negligible effect in combination with long-range disorder such as CI, LRDP and LRDH, but changes the physics dramatically when RS are present. Different sources of disorder can be identified via their fingerprints in the transport and optical measurements, leading to the conclusion that LRDP should be the most common source of disorder in graphene on a substrate.

*Model and Method*— We consider disordered graphene described by the tight-binding (TB) Hamiltonian

$$H = - \sum_{i,j} t_{i,j} c_i^\dagger c_j - \sum_{i,j} t'_{i,j} c_i^\dagger c_j + \sum_i v_i c_i^\dagger c_i, \quad (1)$$

where the first sum is taken over nearest neighbors and the second one - over next-nearest neighbors. For CI, we consider randomly distributed positive or negative point-like charges at the center of a hexagon of the honeycomb lattice ( $\mathbf{r}_k$ )[30], which introduce the Coulomb energy  $v_i = \sum_k \text{sign}(k) e^2 / (\kappa |\mathbf{r}_i - \mathbf{r}_k|)$  at each site  $i$ , and the screening effect due to the substrate is taken into account by using the dielectric constant  $\kappa$  of the substrate. For LRDP, the on-site potential  $v_i$  follows a corrected

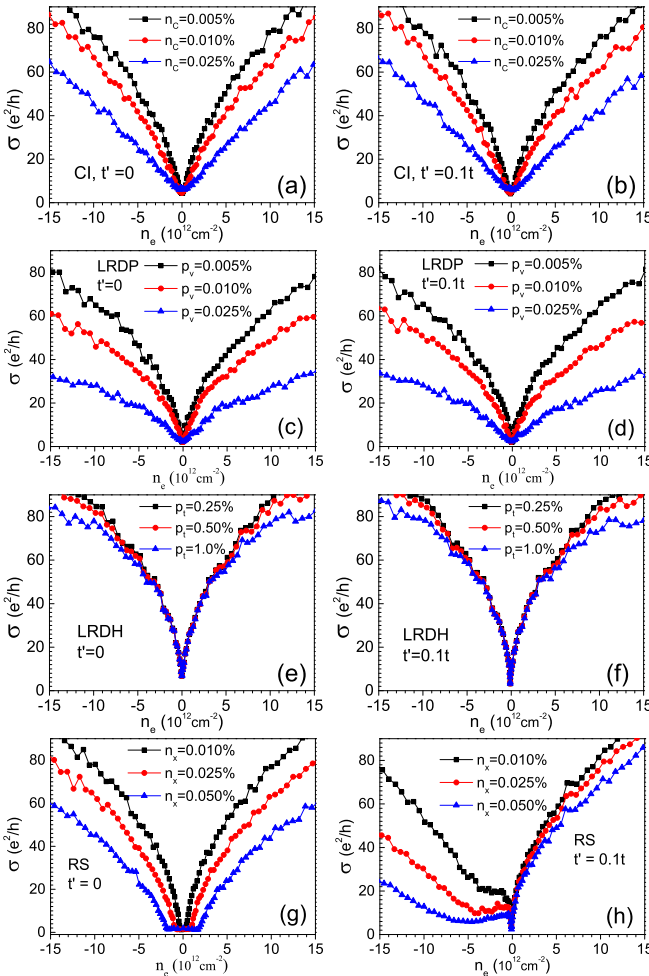


Figure 1. (Color online) The dc conductivity as a function of carrier density  $n_e$  for disordered graphene. Left panels show the results without the NNN hopping  $t'$ , and right panels with  $t' = 0.1t$ . We use  $\kappa = 6$  of hexagonal-boron nitride as a typical value of dielectric constant for graphene on a substrate. Here 0.01% disorder corresponds to a concentration of  $3.82 \times 10^{11} \text{ cm}^{-2}$ .

Gaussian profile which varies smoothly on the scale of lattice constant as  $v_i = \sum_k U_k \exp[-|\mathbf{r}_i - \mathbf{r}_k|^2 / (2d^2)]$  [27], where  $\mathbf{r}_k$  is the  $k$ -th Gaussian centers which are randomly distributed on the lattice with probability  $p_v$ ,  $U_k$  represents the strength of the local potential and is uniformly random in the range  $[-\Delta_v, \Delta_v]$ , and  $d$  is interpreted as the effective radius. We use  $\Delta_v = t$  and  $d = 5a$  to represent the long-range Gaussian potential. Here  $a \approx 1.42 \text{ \AA}$  is the carbon-carbon distance in the single-layer graphene. The LRDH is introduced in a similar way as LRD as the nearest-neighbor hopping parameters are modified according a correlated Gaussian form via  $t_{ij} = t + \sum_k T_k \exp[-|\mathbf{r}_i + \mathbf{r}_j - 2\mathbf{r}_k|^2 / (8d_t^2)]$ , where  $T_k$ ,  $d_t$  and  $p_t$  have similar meanings as in LRD, and we choose  $\Delta_t = 0.25t$  and  $d_t = 5a$  [27]. The

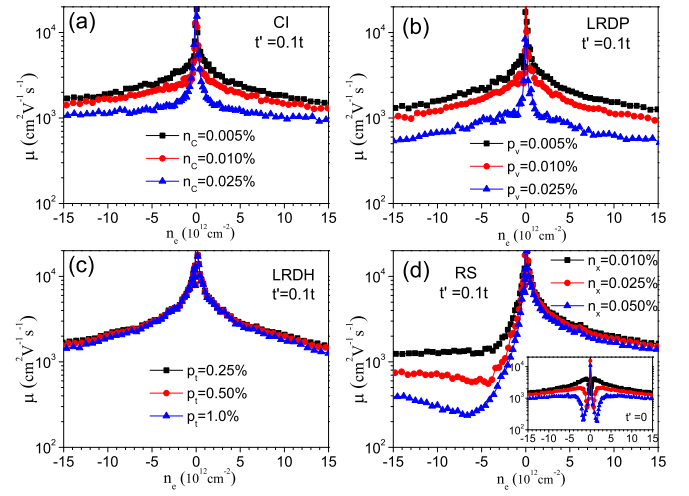


Figure 2. (Color online) The carrier mobility as a function of carrier density  $n_e$  for disorder graphene with  $t'$ . The inner panel in (d) show the results for RS without  $t'$ .

hydrogen-like RS is described by the Hamiltonian  $H_{RS} = V \sum_i (d_i^\dagger c_i + \text{h.c.})$  [11, 31, 32], where  $V$  is the hopping between carbon and adatom. We consider the limiting case with  $V \rightarrow \infty$ , i.e., the electron at the impurity site is completely localized such that the resonant scatterer behaves like vacancy [11]. In our calculations, we use  $t \approx 2.7 \text{ eV}$  and  $t' = t/10$  for the nearest and next-nearest neighbor hopping parameters, respectively. The spin degree of freedom contributes only through a degeneracy factor and, for simplicity, has been omitted in Eq. (1).

The calculations of the electronic and optical properties are performed by the tight-binding propagation method (TBPM) [11, 32–34], which is based on the numerical solution of the time-dependent Schrodinger equation and Kubo's formula. The advantage of this method is that all the calculated quantities are extracted from the real-space wave propagation without any knowledge of the energy eigenstates. Furthermore one can introduce different kinds of (random) disorder by constructing the corresponding TB model for a sample scaling up to micrometers. For more details about the numerical methods we refer to Refs 27 and 32. The simulated graphene sample contains up to  $8192 \times 8192$  atoms subject to periodic boundary conditions.

*Transport properties* — We first consider the carrier-density-dependence of the microscopic conductivity  $\sigma(n_e)$  for disordered graphene. The microscopic conductivity is calculated from the diffusion of the charge transport, without considering the Anderson localization [35–38], and it is comparable to the conductivity extracted from the field-effect measurements. The carrier density  $n_e$  is obtained from the integral of density of states (DOS) via  $n_e(E) = \int_0^E \rho(\varepsilon) d\varepsilon$ . From the results shown in

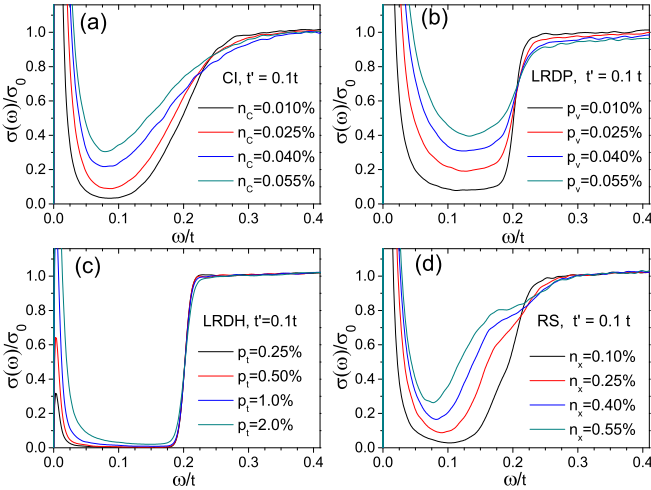


Figure 3. (Color online) The optical conductivity as a function of energy for disordered graphene with  $\mu_F = 0.1t$  and  $t' = 0.1t$ . All along the work the temperature of optical calculation is  $T = 45K$ , the same as in the experiment of Ref. [15].

Fig. 1, we see that (1)  $t'$  is negligible for CI, LRDH and LRDH, and the electron-hole symmetry is preserved, but the results for RS change dramatically. In the presence of RS, there is a strong electron-hole asymmetry in the carrier-density-dependence of dc conductivity. This is due to the fact that the impurity band created by RS is shifted from the Dirac point to the hole side[39], introducing strong electron-hole asymmetry at low energies; (2) as a consequence of this shift the conductivity plateau around the neutrality point is also shifted to the hole side, with an impurity-concentration dependent height and width; (3)  $\sigma(n_e)$  exhibits a sublinear dependence for small concentration for all types of disorder, except for the hole side in RS; (4) For LRDH,  $\sigma(n_e)$  is insensitive to the changes of the disorder concentration ( $p_t$ ).

The field-effect carrier mobility  $\mu$  can be calculated from the conductivity and carrier-density as  $\mu = \sigma/en_e$ . In the following we show only the results with  $t'$  except when RS are present. From the results presented in Fig. 2, we see that (1) the carrier-dependence of mobility  $\mu(n_e)$  is very similar for CI and LRDH; (2) for LRDH,  $\mu(n_e)$  is insensitive to the disorder strength; (3) there is a strong electron-hole asymmetry in  $\mu(n_e)$  when RS are present, that the mobility on the electron side is insensitive to the impurity concentration, and that its value can be one order of magnitude larger than on the hole side. For example, considering a RS concentration of  $n_x = 0.05\%$ , the electron mobility at carrier density  $5 \times 10^{12} cm^{-2}$  is about  $3,000 (cm^2 V^{-1} s^{-1})$  but the hole mobility for the same carrier density is only  $\sim 300$ . This significant difference of the electron and hole mobility is a unique signature of RS; (4) with RS present, on the

hole side, the carrier-density-dependent mobility is not monotonic and  $\mu(n_e)$  reaches a minimum at the density corresponding to the tail of the conductivity plateau. This agrees with the results for the low-mobility samples (K130 and K145) in Ref. [40]. However with RS present and  $t' = 0$ , the drop of mobility at the minimum is one order of magnitude larger than the experimental result.

The minimum conductivity  $\sigma_{\min}$  at the Dirac point is of the order of  $4e^2/h$  for all types of long-range disorders and  $t' = t/10$ . The values of  $\sigma_{\min}$  in CI and LRDH do not depend on  $t'$ , but change with the disorder strength such that larger concentration of disorder leads to larger values of  $\sigma_{\min}$ . This is due to the fact that the increase of potential sources in CI and LRDH will increase the DOS at the  $\mu_F$ , leading to more states which can contribute to the transport. This may also explain the experimental observations in Ref. [40] and [41] in which the low mobility does not necessary correspond to a smaller value of  $\sigma_{\min}$ . For LRDH, the value of  $\sigma_{\min}$  for  $t' = 0$  is about two time larger than the value for  $t' = t/10$ , but both are insensitive to the disorder strength. For RS and  $t' = 0$ ,  $\sigma_{\min}$  is of the order of  $4e^2/\pi h$ , independent on the impurity concentration  $n_x$  [35–38], but if  $t' = t/10$   $\sigma_{\min}$  from being of the order of  $4e^2/h$  at small  $n_x$  to  $4e^2/\pi h$  when  $n_x \geq 0.1\%$ , consistent with the numerical results of Ref. [37] (data not shown). Thus we conclude that our results indicate that the minimum conductivity  $4e^2/h$  found in the experiments are dominated by long-range disorder but that the value of  $4e^2/\pi h$  is due to RS only.

*Optical properties* — As for the transport properties,  $t'$  has negligible effects on the optical properties of disordered graphene, except if RS are present. In general, disorder introduces new states which could contribute to the extra intraband excitations [14, 17–27], and therefore enhances the optical conductivity below  $2\mu_F$ , which might explain the observed background contribution in the optical spectrum for  $0 < \omega < 2\mu_F$  [15, 16]. This is confirmed by the optical conductivity of disordered graphene calculations shown in Fig. 3. For disordered graphene with CI, there is a strong enhancement of the optical conductivity below  $2\mu_F$  and the enhanced spectrum forms a plateau with disorder-dependent minimum conductivity. For LRDH, there is in addition a disorder-dependent plateau in the optical spectrum below  $2\mu_F$ , which is much wider than the one due to CI. For LRDH, the enhancement of the optical conductivity is much smaller than for other types of disorder. For RS and  $t' = 0$ , a disorder-dependent peak appears at  $\omega \approx \mu_F$ , which is due to the enhanced excitations of the midgap states at the Dirac point. This peak disappears for  $t' = t/10$ , and instead, a disorder-dependent narrow plateau appears.

In practice, instead of varying the disorder concentration, it is easier to change the chemical potential by applying an electrical potential to a gate. In order to compare to the experimental data of the spectroscopy mea-

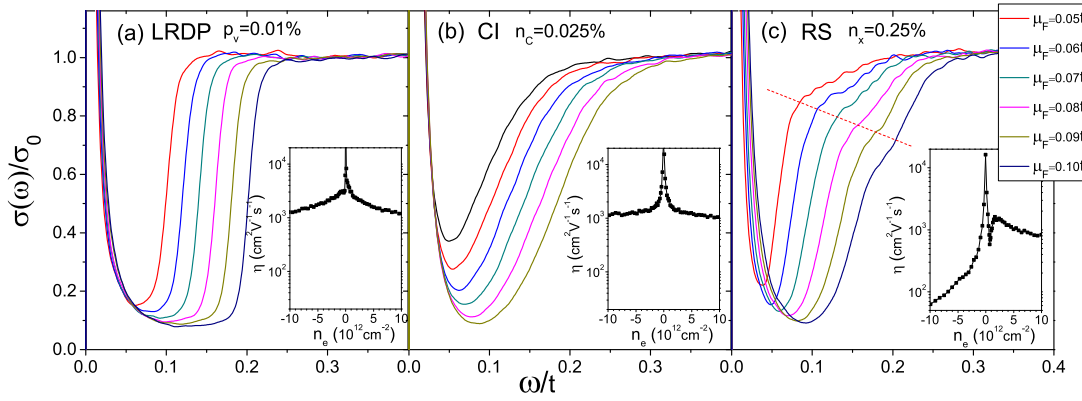


Figure 4. (Color online) The optical conductivity as a function of energy for disordered graphene (a) LRDP, (b) CI, and (c) RS with  $t'$ . The disorder concentrations are determined via the best fit to the experimental results of optical spectroscopy [15, 16]. The chemical potential  $\mu_F$  changes from  $0.05t$  to  $0.1t$ . The inner panels show the corresponding carrier mobility for the same concentration of disorder. The dashed line in (c) is a guide to eye separating two region in which the spectrum changes differently in the presence of RS.

surements [15, 16] quantitatively, we plot in Fig. 4 the best fit of the optical conductivity for different chemical potentials ranging from  $0.05t$  to  $0.1t$ . The disorder concentrations shown in Fig. 4 are determined by matching the minimum value of the optical conductivity plateau to the one observed [15, 16], yielding  $\sigma_{\text{plateau}}$  of the order of  $0.1\sigma_0$  for  $\mu_F \approx t/10$ . The best match of the disorder concentrations from our simulations is  $p_v = 0.01\%$  for LRDP,  $p_c = 0.025\%$  for CI and  $n_x = 0.25\%$  for RS. A direct comparison of the profile of the spectrum between our simulations and the experiments in Ref. [15, 16] indicates that LRDP fits best to the experiments. In Ref. [15], the carrier mobility measured for the same device is as high as  $8,700\text{cm}^2\text{V}^{-1}\text{s}^{-1}$  at carrier densities of  $2 \times 10^{12}\text{cm}^{-2}$ , and the LRDP also gives the highest mobility that it can reach  $\sim 3,000$ . For CI,  $\mu \sim 1500$ , and for RS the mobility is even smaller: for electrons it is  $\sim 1,000$  and for holes  $\sim 300$ . Therefore we conclude that the background contribution of the optical conductivity below  $2\mu_F$  as observed in Ref. [15, 16] should be due mainly to the presence of LRDP.

*Landau level spectrum* — Finally we consider the electronic properties of graphene under a perpendicular magnetic field. The Landau quantization of the energy levels leads to separated peaks, as shown in Fig. 5. In the presence of disorder, the peak amplitudes of the Landau levels (LL) are reduced and the peaks become broader, except for LRDH in which the influence of disorder is much weaker than for other types of disorder. The peak profiles depend on the different sources of disorder. In general, for long-range disorder, the peak is still symmetric along its center, but for RS, the changes are mainly restricted on the side with higher energy. Furthermore, the LL spectrum exhibits electron-hole symmetry for long-range disorder, but becomes asymmetric for RS. Especially, there are two small peaks around the first Landau

level on the hole side shown in Fig. 5(d), which has the same origin as for the zero LL peaks, induced by RS [32]. The differences that appear in the LL spectrum also appear in quantum capacitance measurement, as the inverse of the latter is proportional to DOS [42–45]. Therefore, we also expect a huge effect of RS on the asymmetric quantum Hall conductivity, a topic for future research.

*Conclusion* — We have studied the effects of different types of disorder on the electronic, transport and optical properties of graphene. By comparing the results with and without the NNN hopping, we find that the NNN hopping has negligible effect in combination with long-range disorder such as CI, LRD and LRDH, but that it changes the physical properties dramatically if RS are present. Our results suggest that the different but

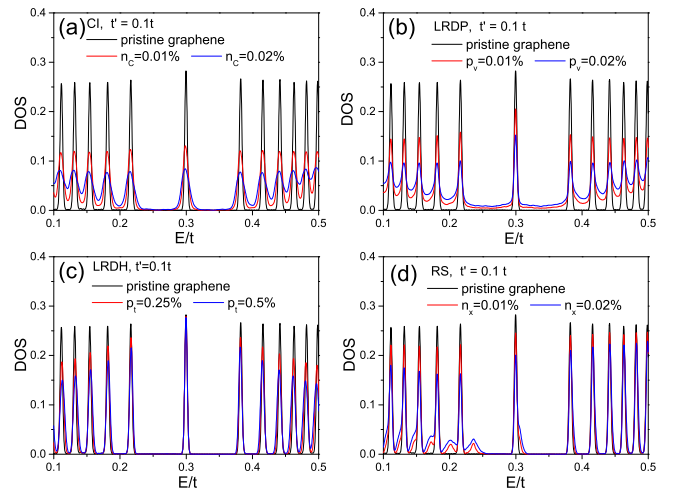


Figure 5. (Color online) Density of states as a function of energy for disordered graphene in the presence of a uniform perpendicular magnetic field ( $B = 50\text{T}$ ).

characteristic features that appear in the calculated electronic, transport and optical properties can be used as fingerprints to identify the dominant sources of disorder in graphene.

*Acknowledgments*— We thank the European Union Seventh Framework Programme under grant agreement n604391 Graphene Flagship. The support by the China Scholarship Council (CSC) and by the Stichting Fundamenteel Onderzoek der Materie (FOM) and the Netherlands National Computing Facilities foundation (NCF) are acknowledged. S.Y. and M.I.K. thank financial support from the European Research Council Advanced Grant program (contract 338957).

\* s.yuan@science.ru.nl

- [1] N. M. R. Peres, Rev. Mod. Phys. **82**, 2673 (2010).
- [2] M. I. Katsnelson, *Graphene: Carbon in Two Dimensions* (Cambridge University Press, 2012).
- [3] L. Ponomarenko, R. Yang, T. Mohiuddin, M. Katsnelson, K. Novoselov, S. Morozov, A. Zhukov, F. Schedin, E. Hill, and A. Geim, Phys. Rev. Lett. **102**, 206603 (2009).
- [4] N. J. G. Couto, B. Sacépé, and A. F. Morpurgo, Phys. Rev. Lett. **107**, 225501 (2011).
- [5] M. Katsnelson and A. Geim, Trans. R. Soc. A **366**, 195 (2008).
- [6] M. Gibertini, A. Tomadin, M. Polini, A. Fasolino, and M. I. Katsnelson, Phys. Rev. B **81**, 125437 (2010).
- [7] M. Gibertini, A. Tomadin, F. Guinea, M. I. Katsnelson, and M. Polini, Phys. Rev. B **85**, 201405 (2012).
- [8] N. J. G. Couto, D. Costanzo, S. Engels, D.-K. Ki, K. Watanabe, T. Taniguchi, C. Stampfer, F. Guinea, and A. F. Morpurgo, Phys. Rev. X **4**, 041019 (2014).
- [9] M. A. H. Vozmediano, M. I. Katsnelson, and F. Guinea, Physics Reports **496**, 109 (2010).
- [10] Z. H. Ni, L. A. Ponomarenko, R. R. Nair, R. Yang, S. Anissimova, I. V. Grigorieva, F. Schedin, P. Blake, Z. X. Shen, E. H. Hill, et al., Nano Letters **10**, 3868 (2010).
- [11] T. O. Wehling, S. Yuan, A. I. Lichtenstein, A. K. Geim, and M. I. Katsnelson, Phys. Rev. Lett. **105**, 056802 (2010).
- [12] M. Orlita and M. Potemski, Semicond. Sci. Technol. **25**, 063001 (2010).
- [13] F. Wang, Y. Zhang, C. Tian, C. Girit, A. Zettl, M. Crommie, and Y. R. Shen, Science **320**, 206 (2008).
- [14] Z. Q. Li, E. A. Henriksen, Z. Jiang, Z. Hao, M. C. Martin, P. Kim, H. L. Stormer, and D. N. Basov, Nature Physics **4**, 532 (2008).
- [15] Z. Li, E. A. Henriksen, Z. Jiang, Z. Hao, M. C. Martin, P. Kim, H. Stormer, and D. N. Basov, Nature Physics **4**, 532 (2008).
- [16] C.-F. Chen, C.-H. Park, B. W. Boudouris, J. Horng, B. Geng, C. Girit, A. Zettl, M. F. Crommie, R. A. Segalman, S. G. Louie, et al., Nature **471**, 617 (2011).
- [17] T. Ando, Y. Zheng, and H. Suzuura, Journal of the Physical Society of Japan **71**, 1318 (2002).
- [18] A. Grüneis, R. Saito, G. G. Samsonidze, T. Kimura, M. A. Pimenta, A. Jorio, A. G. S. Filho, G. Dresselhaus, and M. S. Dresselhaus, Phys. Rev. B **67**, 165402 (2003).
- [19] N. M. R. Peres, F. Guinea, and A. H. Castro Neto, Phys. Rev. B **73**, 125411 (2006).
- [20] V. P. Gusynin, S. G. Sharapov, and J. P. Carbotte, Phys. Rev. Lett. **96**, 256802 (2006).
- [21] T. Stauber, N. M. R. Peres, and F. Guinea, Phys. Rev. B **76**, 205423 (2007).
- [22] V. P. Gusynin, S. G. Sharapov, and J. P. Carbotte, International Journal of Modern Physics B **21**, 4611 (2007).
- [23] T. Stauber, N. M. R. Peres, and A. K. Geim, Phys. Rev. B **78**, 085432 (2008).
- [24] T. Stauber, N. M. R. Peres, and A. H. Castro Neto, Phys. Rev. B **78**, 085418 (2008).
- [25] H. Min and A. H. MacDonald, Phys. Rev. Lett. **103**, 067402 (2009).
- [26] K. F. Mak, M. Y. Sfeir, Y. Wu, C. H. Lui, J. A. Misewich, and T. F. Heinz, Phys. Rev. Lett. **101**, 196405 (2008).
- [27] S. Yuan, R. Roldan, H. D. Raedt, and M. I. Katsnelson, Phys. Rev. B **84**, 195418 (2011).
- [28] A. H. Castro-Neto, F. Guinea, N. M. R. Peres, K. Novoselov, and A. K. Geim, Rev. Mod. Phys. **81**, 109 (2009).
- [29] A. Kretinin, G. L. Yu, R. Jalil, Y. Cao, F. Withers, A. Mishchenko, M. I. Katsnelson, K. S. Novoselov, A. K. Geim, and G. F., Phys. Rev. B **88**, 165427 (2013).
- [30] V. M. Pereira, J. Nilsson, and A. H. Castro Neto, Phys. Rev. Lett. **99**, 166802 (2007).
- [31] J. P. Robinson, H. Schomerus, L. Oroszlány, and V. I. Fal'ko, Phys. Rev. Lett. **101**, 196803 (2008).
- [32] S. Yuan, H. De Raedt, and M. I. Katsnelson, Phys. Rev. B **82**, 115448 (2010).
- [33] A. Hams and H. De Raedt, Phys. Rev. E **62**, 4365 (2000).
- [34] S. Yuan, T. O. Wehling, A. I. Lichtenstein, and M. I. Katsnelson, Phys. Rev. Lett. **109**, 156601 (2012).
- [35] A. Cresti, F. Ortmann, T. Louvet, D. Van Tuan, and S. Roche, Phys. Rev. Lett. **110**, 196601 (2013).
- [36] G. Trambly de Laissardière and D. Mayou, Phys. Rev. Lett. **111**, 146601 (2013).
- [37] G. T. de Laissardière and D. Mayou, Advances in Natural Sciences: Nanoscience and Nanotechnology **5**, 015007 (2014).
- [38] S. Yuan, R. Roldán, M. I. Katsnelson, and F. Guinea, Phys. Rev. B **90**, 041402 (2014).
- [39] V. M. Pereira, J. M. B. Lopes dos Santos, and A. H. Castro Neto, Phys. Rev. B **77**, 115109 (2008).
- [40] Y.-W. Tan, Y. Zhang, K. Bolotin, Y. Zhao, S. Adam, E. H. Hwang, S. Das Sarma, H. L. Stormer, and P. Kim, Phys. Rev. Lett. **99**, 246803 (2007).
- [41] A. Geim and K. Novoselov, Nat. Mat. **6**, 183 (2007).
- [42] T. Fang, A. Konar, H. Xing, and D. Jena, Appl. Phys. Lett **91**, 092109 (2007).
- [43] J. Xia, F. Chen, J. Li, and N. Tao, Nature Nanotech. **4**, 505 (2009).
- [44] S. Dröscherscher, P. Roulleau, F. Molitor, P. Studerus, C. Stampfer, K. Ensslin, and T. Ihn, Appl. Phys. Lett **96**, 152104 (2010).
- [45] L. Wang, X. Chen, W. Zhu, Y. Wang, C. Zhu, Z. Wu, Y. Han, M. Zhang, W. Li, Y. He, et al., Phys. Rev. B **89**, 075410 (2014).